Bioconjugate Chemistry

Review

pubs.acs.org/bc

Upconversion Nanoparticles: A Versatile Solution to Multiscale Biological Imaging

Xiang Wu,[†,‡] Guanying Chen,[§,∥] Jie Shen,*[,†] Zhanjun Li,[†] Yuanwei Zhang,[†] and Gang Han*[,†]

[†]Department of Biochemistry and Molecular Pharmacology, University of Massachusetts Medical School, Worcester, Massachusetts 01605, United States

[‡]State Key Laboratory of Fine Chemicals, Dalian University of Technology, Dalian, Liaoning 116012, China

[§]School of Chemical Engineering and Technology, Harbin Institute of Technology, Harbin, Heilongjiang 150001, China

[∥]Department of Chemistry and the Institute for Lasers, Photonics, and Biophotonics, University at Buffalo, State University of New York, Buffalo New York 14260, United States

ABSTRACT: Lanthanide-doped photon upconverting nanomaterials are emerging as a new class of imaging contrast agents, providing numerous unprecedented possibilities in the realm of biomedical imaging. Because of their ability to convert long-wavelength near-infrared excitation radiation into shorter-wavelength emissions, these nanomaterials are able to produce assets of low imaging background, large anti-Stokes shift, as well as high optical penetration depth of light for deep tissue optical imaging or light-activated drug release and therapy. The aim of this review is to line up some issues associated with conventional fluorescent probes, and to address the recent advances of upconverting nanoparticles (UCNPs) as a solution to multiscale biological imaging applications.

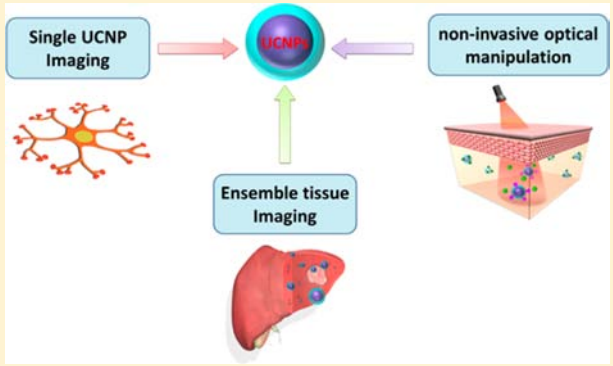

1. INTRODUCTION

Optical imaging is one of the most facile and straightforward ways to investigate biomedical specimens.[1] To improve imaging signal contrast and spatial resolution, various optical probes have been developed in the past decades,[2] which can pinpoint the position of prescribed biomolecule targets. Especially, the classic category of fluorescent probes, such as fluorescent dyes,[3] fluorescent proteins,[4] and quantum dots (QDs),[5] have drawn a great deal of attention from both chemistry and biology scientists. Thanks to these fluorescent probes, some secrets of life from downward at the single molecular scope to upward at the in vivo tissue level are able to be visualized.[6] However, these well-established fluorescent probes are experiencing certain incompetence when tackling the puzzles with ever-elevating difficulties and complexities in life science.[7] For instance, a single molecular study is severely limited by the problems of insufficient intensity and fast photobleaching of fluorescent probes,[8] while in vivo fluorescent optical imaging suffers from a strong background of autofluorescence and light scattering as well as a limited imaging depth.[9] The demands for new fluorescent probes with higher brightness, photostability, and spectral distinguishability for bioimaging[10] never end.

Lanthanide-doped upconverting nanoparticles (UCNPs) are emerging as a new class of optical probes, which hold great promise to overcome the inborn shortcomings associated with dyes, fluorescent proteins, and QDs.[11] The emission phenomenon from UCNPs is, by appearance, a little similar to multiphoton-excited fluorescence from conventional biolabels (such as dyes and QDs), since both of them are produced by converting long-wavelength excitation photons into shorter-wavelength emission photons.[12] It is noted that simultaneous multiphoton excitation has been widely applied in fluorescent optical microscopy to show increased resolution, decreased specimen autofluorescence, as well as increased imaging depth.[13] However, the low NIR absorption cross section of multiphoton labels requires this technique to subject to the use of high-peak-power ultrashort-pulsed laser. Moreover, the photobleaching and/or photoblinking problem persists for dyes or QDs in multiphoton microscopy, and the high peak power of the femto or pico pulsed laser used can produce possible photodamage in biological specimens.[14] Principally distinct from simultaneous multiphoton process in dyes and QDs, which involves the use of a virtual energy level, photon upconversion in UCNPs relies on the sequential absorption of low energy photons through the use of ladder-like energy levels of lanthanide doping ions.[15] This quantum mechanical difference makes UCNPs orders of magnitude more efficient than multiphoton process, thus allowing excitation with a low-cost continuous-wave laser diode at low-energy irradiance; typically as low as $\sim 10^{-1}$ W.cm^{-2}.[16] UCNPs also have other superior advantages for probe uses in imaging, as shown in Table 1. First, the intra f−f electronic transitions of Ln dopants

Received: August 25, 2014
Revised: September 23, 2014
Published: September 25, 2014

   dx.doi.org/10.1021/bc5003967 | *Bioconjugate Chem.* 2015, 26, 166−175

Table 1. Photochemical and Photophysical Parameters Showing the Advantages of UCNPs in Imaging Compared to Dyes and QDs

parameter	days	QDs	UCNPs
emission fwhm	50 nm	20−50 nm	<20 nm
decay magnitude	1 ns	10 ns	100 μs
photobleaching	fast	slow	none
photoblinking	yes	yes	no
multiphoton excitation power (W/cm^2)	10^6−10^9	10^4−10^6	1−10^3

produce a set of atomic-like line emission peaks from UCNPs. These sharp emissions are able to reduce the possibilities of spectra overlapping, and facilitate the retrieval of signal during signal screening process. Second, the parity-forbidden nature of intra f−f transitions produces a long UC luminescence decay (up to 10 ms), providing opportunities for time-resolved imaging, biosensing, and multiplexing. Third, the intra f−f electron transitions are well-shielded by the outer complete 5s and 5p electron shells, thus resisting oxidation-induced photobleaching that is often seen for electronic transitions of organic dyes. Fourth, due to a collective emission of abundant dopants within a single UCNP, luminescence from a single UCNP does not show the blinking behavior, which is important for single molecule imaging experiments involving a long-time observation.[17] These unique and fascinating properties of UCNPs will offer realistic resolutions to address the challenges met in single molecule level, as well as in deep tissue optical imaging level. It also inspires manipulation of various photochemical reactions in vivo using biocompatible and captivating NIR light in conjunction with the frequency converting ability of UCNPs.

In this Review, as illustrated in Scheme 1, we will cover four aspects of UCNPs from their recent advances: (i) a brief introduction to UCNPs; (ii) single nanoparticle imaging; (iii) ensemble optical imaging, encompassing in vitro cell culture imaging, deep tissue optical imaging, as well as multimodal animal bioimaging; (iv) NIR light mediated photochemistry and phototherapy. We will also present our own views in regard to the future directions for UCNPs in the Conclusion section.

Scheme 1. Overview of the Present Tutorial Review

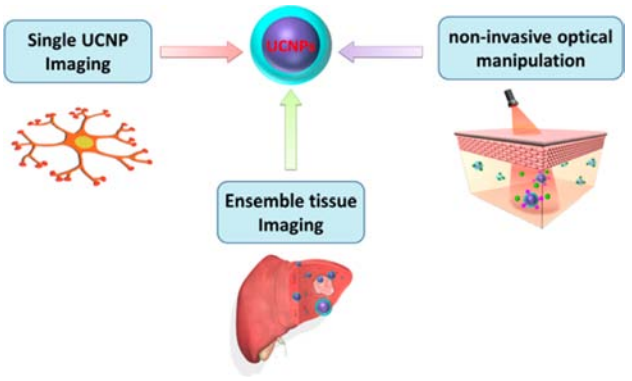

2. INTRODUCTION OF UCNPS

2.1. UC Phenomenon. Photon upconversion is characterized by the conversion of long-wavelength radiation, for instance, infrared or near-infrared (NIR) radiation, to short-wavelength emissions. The upconversion could take place by several different mechanisms, which have been summarized and discussed in detail in several review articles.[18] Typically, realization of the UC phenomenon requires a proper host lattice selected lanthanide dopants of sensitizer and activator, and an excitation source of appropriate wavelength (Figure 1).

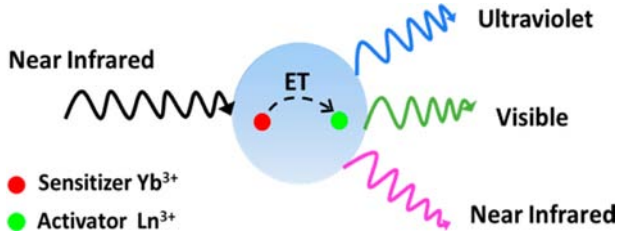

Figure 1. Schematic representation of the excitation/emission and interatomic energy transfer profiles of UCNPs.

The host lattice determines the spatial distribution, coordination number, as well as the type of surrounding anions of the dopants. An ideal host material should have low lattice phonon cutoff energies to minimize nonradiative energy losses in the intermediate states, thus maximizing the output of radiative emission. To date, $NaYF_4$, $NaYbF_4$, $NaGdF_4$, $NaLaF_4$, $NaLuF_4$, $LiYF_4$, $LiLuF_4$, LaF_3, YF_3, GdF_3, GdOF, La_2O_3, Lu_2O_3, Y_2O_3, Y_2O_2S, and others have been identified as competent UC host materials. The Ln^{3+} with ladder-like arrangement energy levels, such as Er^{3+}, Tm^{3+}, and Ho^{3+}, are typically used as activator dopants, while the Yb^{3+} is often codoped as the sensitizer to enhance the resulting UC efficiency. The Yb^{3+} sensitizer has only two distinct energy levels, permitting an exclusive strong absorption at ∼980 nm that coincides with the output of NIR laser diodes.

2.2. Synthesis and Functionalization of UCNPs. Much earlier than the arise of UCNPs, UC phenomena have been established in bulk materials with numerous combinations of host and Ln^{3+} dopants, yet only a few combinations are able to reproduce UC phenomena in the form of colloidal nanocrystals (i.e., UCNPs) mainly due to the synthetic problems, as well as nanosize-induced low emission efficiency. Typically, fluoride-based lattices, such as $NaYF_4$, have been extensively used as an UCNP host material because of their relatively low phonon energy (i.e., 350 cm^{-1}), high optical transparence, and good crystallinity under mild synthesis temperature. A range of synthetic approaches such as thermal decomposition, hydro-(solvo)thermal synthesis, sol−gel processing, coprecipitation method, as well as ionic liquid-based synthesis have been investigated to synthesize high-quality lanthanide-doped $NaYF_4$ UCNPs with controlled stoichiometric composition, crystalline phase, and morphology. In particular, thermolysis[19] and solvothermal method[20] are the two most widely used methods, as they can produce precise control over the phase, shape, size, and stoichiometric composition of the core only and/or the core/shell UCNPs.

To produce high crystallinity and uniform morphology of UCNPs, the aforementioned synthesis strategies are usually carried out in high-boiling-point (nonaqueous) solvents in association with one or two appropriate long-chain ligands. As a result, the synthesized UCNPs are generally capped by hydrophobic ligands (such as oleic acid). Thus, water solubilization and/or bioactive/inert functionalization are two further critical steps to empower UCNP to serve as a reliable nanoplatform in biological applications. General strategies

dx.doi.org/10.1021/bc5003967 | Bioconjugate Chem. 2015, 26, 166−175

include ligand removal,[21] ligand exchange,[22] ligand oxidation,[23] polymer coating,[24] silica coating,[25] and layer-by-layer deposition.[26] Details of these pertinent procedures can be found in the recent review.[7]

3. SINGLE MOLECULE LEVEL IMAGING

Single UCNP Imaging. The development of optical probes for single molecule imaging has boosted the subcellular study of single molecule events in cells. An ideal single-molecule probe should exhibit good brightness, uninterrupted emission, resistance to photobleaching, and minimal spectral overlap with cellular autofluorescence. Despite significant improvements in software and methodology for microscopic imaging in the past decade, the currently available single molecule probes (such as dye and protein) are problematic with respect to the following characteristics: lack of superior brightness, uninterrupted emission (no blinking), resistance to photobleaching, and minimal spectral overlap with cellular autofluorescence (consult Table 1).

One key requirement when using nanoparticles to image a single molecule behavior is that they must be size-compatible with the biomolecules so as not to produce interference on bioactivity of the labeled biomolecule. To this end, several kinds of nanoparticles in the size range of ~4−10 nm have been developed and used for such a purpose, such as gold nanoparticles, semiconductor QDs, and nanodiamonds. In particular, QDs have been frequently used for molecular imaging due to their superior brightness. Yet, single/near single QDs have a time-dependent emission that goes on and off, in other words, a "blinking" problem. The blinking dynamics of a QD is essentially random and cannot be predicted. Thus, although the pros and cons for blinking are not absolute, a QD trajectory cannot last indefinitely and an off-state of blinking can kill the trajectory instantly.

Single UCNP imaging was first proposed and demonstrated by Han et al.[24] UCNPs are ideal for single-molecule imaging due to five unique features: (1) Unlike Stokes-shifted luminescence from organic- and protein-based fluorophores or semiconductor QDs, anti-Stokes luminescence of UCNP circumvents autofluorescence imaging background. (2) They are completely nonblinking and exceptionally photostable, allowing for long-term tracking of biomolecules. Moreover, they are orders of magnitude more efficient than conventional two-photon processes. (3) The utilization of noninvasive NIR excitation can minimize cell damage as well as the scattering imaging background. (4) All the individual UCNPs are bright; no dark nanoparticles exist. (5) Strong upconverting signals can be detected against a virtually zero background in the context of cells (Figure 2). In 2011, Suh et al. reported the first real-time tracking study with UCNPs at the single vesicle level in a living cell; intracellular movements of UCNPs were able to be visualized for as long as 6 h without interruption.[27]

Single UCNP imaging has become increasingly available in biology; however, the involved UCNPs often have a size of ~20−30 nm that is larger than most big biomolecules, such as proteins. Preparation of smaller-sized UCNPs but retaining the exceptional optical properties had met with limited success. In this regard, Cohen et al. systematically adjusted several factors that influence the size of UCNPs using a nanocrystal-making robot.

These factors include the crystalline phase of the host matrix, reaction time, and temperature as well as the compositions and ratios of reaction precursors. They identified reactions that

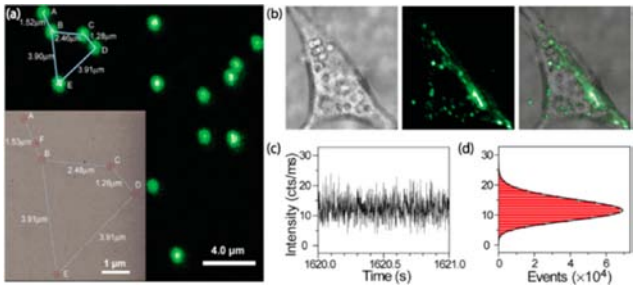

Figure 2. (a) Confocal upconverted luminescent image of individual UCNPs. (b) Live-cell imaging of UCNPs in NIH 3T3 murine fibroblasts, showing virtually zero autofluorescence background. (c,d) Zoom-in time trace and histogram of emission intensity, showing no on/off behavior-nonblinking. (Reprinted with permission from ref 20. Copyright 2009 Highwire press PNAS.)

permit the synthesis of Ln-doped hexagonal phased $NaYF_4$ nanocrystals with controlled diameters ranging from 4.5 to 15 nm.[28] These ultrasmall nanocrystals (<1/4 the diameter of previously characterized UCNPs) retain their continuous emission and photobleaching resistance (Figure 3), so those single particles of sub 10 nm diameter were able to be successfully imaged when excited using a ~980 nm continuous-wave laser irradiance.

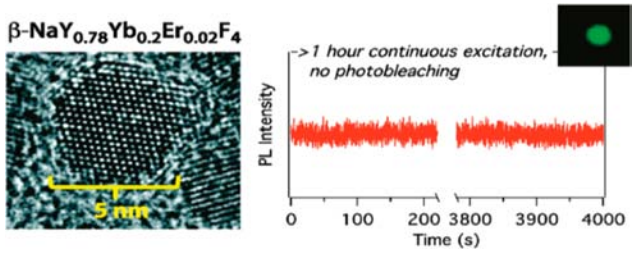

Figure 3. (left) TEM micrograph of 4.5 nm ultrasmall UCNP; (right) time trace showing no blinking. (Reprinted with permission from ref 24. Copyright 2012 American Chemical Society.)

Although the sub 10 nm size is compatible with many imaging applications, the reduction in size significantly diminishes the brightness, because surface energy losses are increased due to the amplified surface to volume ratio, and the number of sensitizer and emitter ions per particle are also reduced. Recently, Cohen et al. developed upconverting nanoparticles with sub 10 nm diameter, yet are over an order of magnitude brighter than existing compositions under single-particle imaging conditions. Single UCNP as small (d = 4.8 nm) as fluorescent proteins was still able to be visualized.[29]

They showed that, for single-molecule studies, emitter concentrations should be as high as possible without compromising the structure of the nanocrystal, while the sensitizer content becomes less significant under high laser irradiance (~10^6 W/cm^2) and can potentially be eliminated for single-molecule imaging applications. To validate this assumption, they synthesized a series of 8 and 5 nm UCNP with either higher emitter or lower activator content, and compared the brightness employing laser irradiance in a single-particle experiment. They observed that the conventional Yb^{3+}/Er^{3+}-codoped UCNPs indeed are brighter than single high-Er^{3+} doped UCNPs at lower powers. As excitation powers are raised, the conventional UCNPs saturate in brightness while the high-Er^{3+} doped UCNPs continue to increase in brightness, finally

dx.doi.org/10.1021/bc5003967 | Bioconjugate Chem. 2015, 26, 166−175

surpassing the conventional UCNPs. The excitation intensity at which $NaYF_4$:20% Er^{3+} UCNPs become brighter than conventional $NaYF_4$:20% Yb^{3+}, 2% Er^{3+} counterparts are ~3 × 10^5 $W.cm^{-2}$. This concludes that even smaller UCNPs may be viable as single-molecule probes. They further prepared 5.5-nm-diameter β-$NaYF_4$ UCNPs doped with 20% Er^{3+} and no Yb^{3+} sensitizer, as well as 4.8 nm UCNPs doped with 20% of Er^{3+} and 20% Yb^{3+}. They found that both UCNPs are significantly brighter than the canonical β-$NaYF_4$:20% Yb^{3+}, 2% Er^{3+} nanocrystals of a similar size.

Similarly, Jin et al. demonstrated a novel approach to significantly enhance the upconverting luminescence of nanocrystals, by increasing the activator concentration from 0.5 mol % to 8 mol % Tm^{3+} in $NaYF_4$ in combination with an elevated irradiance excitation (~1 × 10^6 W/cm^2).[30] The microstructure photonic fiber dip sensor used can easily achieve such high excitation intensities. They showed that even a single nanoparticle can be detected when entering the phototonic fiber from the other end, providing new possibilities to implement high-sensitivity remote biosensing. Highly Ln^{3+}-doped nanoparticles in conjuction with sufficient irradiance excitation have strong potential for use as photostable, background-free, and extremely bright probes for single molecule imaging.

4. ENSEMBLE OPTICAL IMAGING

4.1. In Vitro Imaging. *4.1.1. Multicolor Emission for Bioassays.* Fabricating multicolor assays based on UCNPs is of particular importance for bioimaging and real-time tracking of multiple targets, such as the systems of proteins and genes. A number of strategies have been used to fulfill the multicolor output of UCNPs, such as (1) modulating component species and ratio; (2) adjusting appropriate energy transfer pathways; (3) adapting energy transfer to organic dyes or quantum dots.[7] Among others,[31] Chen and Han fabricated a series of ultrasmall (3.7 nm) YF_3 nanocrystals doped with Yb^{3+}/Er^{3+}, Yb^{3+}/Tm^{3+}, and $Yb^{3+}/Er^{3+}/Tm^{3+}$. By changing the Yb^{3+} doping concentrations in order, the interaction between sensitizer and the activator was tailored, and as a result the output colors were harnessed (Figure 4).[32]

Yb^{3+}/Er^{3+} codoped $NaYF_4$ UCNPs have an intense green emission around 550 nm and a weak dark red emission around 660 nm. While the dark red emission falls on the edge of "optical transparency window of tissue" and thus is preferred for in vivo imaging studies, the weak intensity impedes such applications. To enhance the red emission output while suppressing the generation of green emission, Gu and Zhao prepared $NaYF_4$:Yb^{3+}/Er^{3+} UCNPs tridoped with Mn^{2+} ions. The coexistence of Mn^{2+} disturbs the pathway of generating green emission and facilitates the possibilities of red emission, and thus, the obtained 30% Mn^{2+} doping resulted in a bright pure red emission.[33]

4.1.2. Cellular Imaging. High contrast cellular imaging has been widely reported in recent years using developed multicolored UCNPs. It has been shown that surface modification using targeting molecules such as folic acid (FA), biotin, antibodies, and peptides can lead to improved cellular uptake and enhanced intracellular imaging due to receptor-mediated endocytosis. The ability of UCNPs to target cancerous cells produces opportunities to diagnose the tumors inside the bodies.

One of the first demonstrations of UCNPs for cellular imaging was reported in 2008 by Zhang et al., who

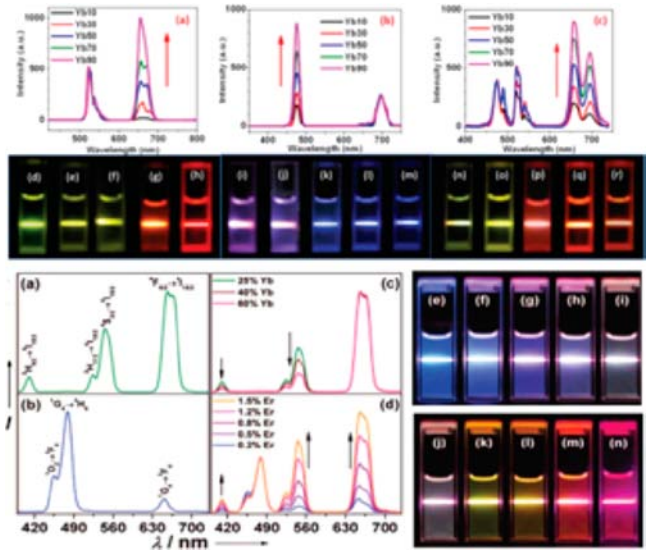

Figure 4. Compiled luminescent spectrum and photos showing corresponding colloidal solution of series of Ln^{3+}-doped nanoparticles. (Reprinted with permission from refs 27 and 28. Copyright 2014 American Chemical Society and 2012 Royal Society of Chemistry Publishing.)

demonstrated that polyethylenimine (PEI)-coated $NaYF_4$:Yb^{3+}/Er^{3+} UCNPs conjugated with folic acid were able to target human HT29 adenocarcinoma cells and human OVCAR3 ovarian carcinoma cells that overexpressed folate receptors on the cell surface.[34] Similarly, Wang and co-workers demonstrated that amino-modified $NaYF_4$:Yb,Er UCNPs were linked to the rabbit anti-CEA8 antibody to form the antibody−UCNP conjugates by a simple route, and the antibody−UCNP conjugates were used as fluorescent biolabels for the effective and time-efficient immunolabeling and imaging of HeLa cells. Strong fluorescence signal from the UCNPs was observed over the cell membrane, but no autofluorescence from the cell was found under 980 nm NIR light excitation.[35]

4.1.3. Deep Tissue Imaging. Compared to visible UC emission, the NIR UC emission are more interesting in deep tissue imaging, as both excitation and emission wavelengths fall within the biological NIR optical transmission window (700−1000 nm). High-contrast deep tissue optical imaging is allowed using NIR_{in}-NIR_{out} UCNPs, as biological tissue will show much lower NIR light attenuation and scattering effects, and auto fluorescence is absent when collecting the NIR UC emission. Prasad and co-workers first reported high-contrast in vitro and in vivo bioimaging using NIR_{in}-NIR_{out} $NaYF_4$:Yb^{3+}/Tm^{3+} UCNPs.[36] In order to improve the UCNPs' efficiency, the same group by Prasad and co-workers established a novel strategy that not only results in an 8-fold enhancement of the quantum yield, but also increases the extinction coefficient of every nanoparticle 5 times by elevating the concentration of the sensitizer Yb^{3+}.[37] In 2013, Yan et al. reported on the use of biocompatible material of CaF_2 to encapsulate UCNPs cores, displaying emissions 4−5 times stronger than the one coated with a traditional $NaYF_4$ inert shell. Using the same strategy, Han et al. developed $NaYbF_4$:Tm^{3+}/CaF_2 UCNPs and used for whole-body mice imaging. An imaging depth as high as ~3.2 cm was demonstrated using biological tissue (pork tissue) as a model. Moreover, high-contrast UC imaging of deep tissues was demonstrated by using a nanoparticle-loaded synthetic fibrous mesh wrapped around rat femoral bone; 7 days after the

dx.doi.org/10.1021/bc5003967 | Bioconjugate Chem. 2015, 26, 166−175

UCNP-loaded mesh was implanted, the operated hind leg was imaged (Figure 5).[38]

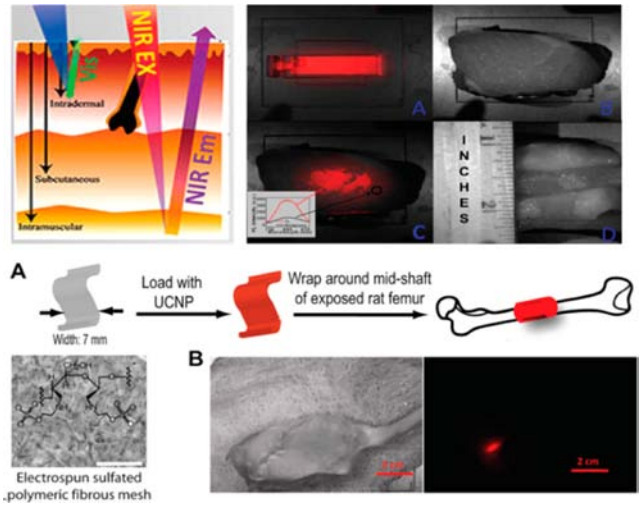

Figure 5. (top) left: the tissue depth of NIR and visible light. right: (a) UCPL bright-field image of a cuvette filled with a suspension of the core/shell nanoparticles, (b) bright-field image of a cuvette covered with pork tissue with a quarter coin stood aside showing its thickness, (c) merged UCPL/bright-field image of the cuvette covered with pork tissue, and (d) bright-field image of the pork tissue (side view). The inset in (c) shows the spectra obtained from the circled areas. (bottom) Polyethylenimine-coated NIR_{in}-NIR_{out} R-(NaYbF4:0.5% Tm_3t)/CaF_2 core/shell nanoparticles for imaging a synthetic periosteal mesh implanted around a rat femur. (a) UCNPs were loaded on a 7-mm-wide sulfated polymer mesh and wrapped around the mid shaft of a rat femur. Scale bar: 500 μm. (b) Bright-field image of the rat hind leg after closing muscle/skin by suture (left) and PL image (right) of the deeply embedded UCNP-stained synthetic mesh wrapped around the rat femur. Scale bar: 2 cm. (Reprinted with permission from ref 34. Copyright 2012 American Chemical Society.)

4.2. Multimodal Small Animal Imaging. Small animal imaging, especially in vivo imaging, is able to provide important information on the pathogenesis, progression, and treatment of many human diseases, which is of vital significance in the study of biology and medicine. Various imaging technologies, such as single-photon emission computed tomography (SPECT), magnetic resonance imaging (MRI), and fluorescence imaging, have been developed to obtain the structural and functional information on biological systems. Among these imaging techniques, luminescence imaging offers a simple but powerful and versatile tool for the visualization of both structural and functional information ranging from living cell to animal level. Recently, upconversion luminescence imaging of small animals has received increasing attention due to its ability to obtain anatomical and physiological details of living systems. Owing to their unique NIR excited anti-Stokes luminescence properties, unified UCNPs have found diverse applications in tumor imaging, vasculature imaging, brain imaging, and multimodal imaging.[14]

Detection of life-threating tumors is considered to be one of the most important applications of optical nanoprobes. In spite of the fast development toward this regard, imaging of small tumors, especially tiny tumors (1−4 mm), still remains a challenge. Typically, small tumors have a geometric resistance which is lower than the large tumors against a blood flow. As a result, it is more difficult for nanoparticles to absorb in small tumors than in big tumors due to the higher blood flow rate. This probably constitutes the reason that most nanoprobe-based tumor imaging results achieved so far have been on tumors with a size ranging from 5 to 15 mm. Liu and co-workers reported imaging results of tiny tumor with a diameter smaller than 2 mm utilizing an antibody (monoclonal anti-EGFR antibody) modified PEGylated $NaGdF_4$:Yb^{3+}/Er^{3+} UCNPs.[39] Specifically, combined MRI and UC luminescence imaging was performed to image intraperitoneal tumors and subcutaneous tumors in vivo. A subcutaneous tumor ∼1.7 mm × 1.9 mm was clearly visualized through the green upconversion luminescence. Pharmacokinetic studies revealed a size-dependent elimination pathway. A biliary elimination pathway was taken by larger UCNPs ∼18.5 nm excreting more than 87% of the particles after 30 days postadministration, while both renal and biliary clearance pathways were adopted by smaller UCNPs ∼5.1 nm resulting in a greatly shortened biological half-time.

Up to now, various imaging modalities have been developed for diverse applications. However, no single imaging modality can meet all the requirements either for scientific research or practical application, since each imaging modality has its own advantages and disadvantages. For example, SPECT is highly sensitive and quantitative, but limited by the resolution (micrometer level) and the inability to provide anatomical information. MRI and CT are suitable for anatomical reconstruction but lack the ability to provide molecular information. Fluorescence optical imaging is suitable for multiscale imaging from the cellular level to the whole-body animal but is hindered by the limited imaging depth of less than several centimeters according to up-to-date reports. Bioimaging using multimodalities in a single nanoplatform is able to overcome the limitations of single imaging modality, and then provide more abundant and complementary information to improve the accuracy of diagnostics. Thus, the fabrication of multimodal imaging nanoprobes with upconversion properties has become one of the most important developing directions of UCNPs. In this regard, Li's group has made lots of constructive contributions such as dual-modal, trimodal imaging, by carefully integrating diverse properties of various elements into single particle. Recently, Li's group reported on $NaLuF_4$:Yb,Tm@ $NaGdF_4$ (^{153}Sm) core@shell nanocomposites which allowed achievement of CT, MRI, SPECT, and upconversion luminescence four-modal imaging in a mouse model (Figure 6).[40] The use of multimodal nanoprobes entails collection of abundant information at the same time including the biodistribution in different tissues and organs, the dynamic long-term quantification data, as well as the 3D information on a body.

Angiogenesis, the formation of new blood vessels from the preexisting vasculature, is essential for tumor growth and progression. Esipova and co-workers reported cortical vasculature imaging in mouse brain by using UCNPs with surface modification by polyanionic dendrimer.[41] These polyglutamic dendritic UCNPs dissolved in the blood allowed mapping of the brain cortical vasculature down to 400 μm under the tissue surface. Owing to the high efficiency of UCNPs, laser photon flux almost 10^6 times lower than that typically used in two-photon imaging was involved to perform the excitation to reach high-resolution depth-resolved imaging of brain tissue.

Glioblastoma are typical malignant tumors on the supportive tissue of the brain; the cancerous cells reproduce quickly and its

dx.doi.org/10.1021/bc5003967 | Bioconjugate Chem. 2015, 26, 166−175

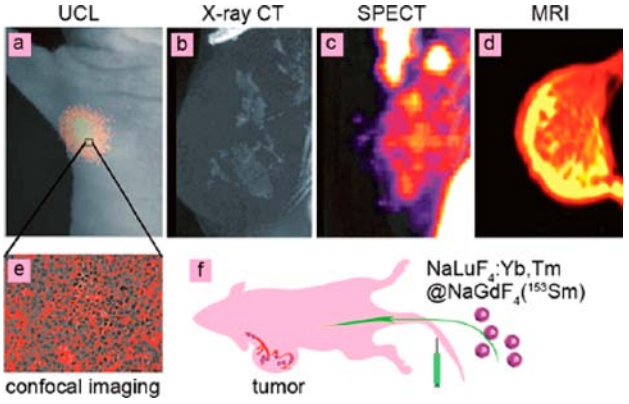

Figure 6. Four-model imaging of the focused tumor from the tumor-bearing nude mouse 1 h after intravenous injection of $NaLuF_4$:Yb,Tm@$NaGdF_4$(^{153}Sm): (a) In vivo UCL-image, (b) X-ray CT image, (c) SPECT image, (d) MR image of tumor. (e) UCL confocal image of the paraffin section of tumor tissue. (f) Schematic illustration of tumor angiogenesis imaging using aLuF_4:Yb,Tm@$NaGdF_4$(^{153}Sm) as the probe. (Reprinted with permission from ref 36. Copyright 2013 American Chemical Society.)

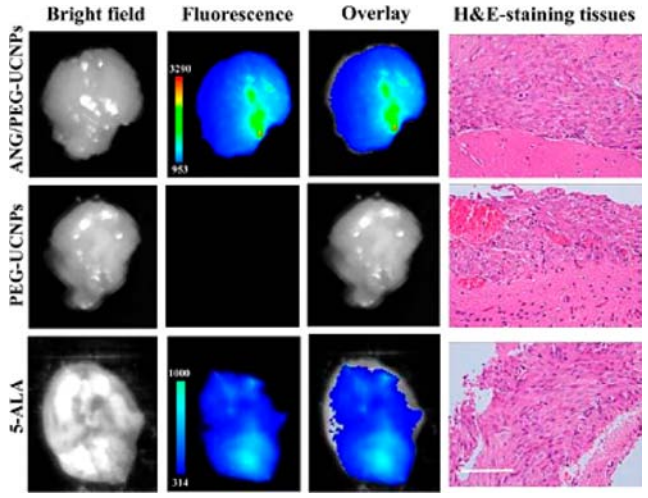

Figure 7. Ex vivo fluorescent images of glioblastoma-bearing brain in 1 h after the intravenous injection with ANG/PEG-UCNPs, PEG-UCNPs (excitation, 980 nm; emission, 800 nm), and 5-ALA (excitation, 470 nm; emission, 650 nm). All imaging experiments were performed under the same condition. H&E-staining of the tumor tissues from glioblastoma-bearing mice brain was used to demonstrate the existence of glionblastoma. Scale bar: 100 μm. (Reprinted with permission from ref 38. Copyright 2014 American Chemical Society.)

growth is supported by a large network of blood vessels. Surgical resection bears the potential risk of incomplete excision due to the inherent infiltrative character of the glioblastoma. Present contrast agents suffer from poor blood-brain barrier permeability and non-targeting-specificity, resulting in the risk of inefficient diagnosis and resection of glioblastoma. Ni and co-workers developed a dual-targeting $NaYF_4$:Yb/Tm/Gd@$NaGdF_4$ nanoprobe to cross the blood-brain barrier (BBB). Angiopep-2 was covalently bound to PEGylated UCNPs, which allowed a receptor-mediated transcytosis (to cross BBB) and subsequently targeted the glioblastoma. Moreover, the Angiopep-2/PEG-UCNPs bimodal nanoprobes showed a great potential in preoperative diagnosis and intraoperative positioning of the brain tumors by MR and NIR-to-NIR upconversion imaging, outperforming the clinically used MRI contrast Gd-DTPA and fluorescent dye 5-aminolevulinic acid (Figure 7).[42]

4.3. New Excitation Wavelengths for Ensemble Imaging. Even though deep tissue penetration and high contrast imaging have been achieved by using conventional UCNPs, they are typically excited at ~980 nm which coincides with the extinction of water. Thus, high laser irradiance or long time irradiation at ~980 nm could lead to a temperature rise and consequently induce tissue damage. Shifting of the excitation to other NIR wavelengths to preclude possible heating effect would be appealing for bio applications. Excitations at 900−1000 nm for Yb^{3+} and 1522 nm for Er^{3+} have been reported. Moreover, Han et al. designed UCNPs tridoped with the absorber Nd^{3+}, the sensitizer Yb^{3+}, and the activator Er^{3+} (or Tm^{3+}) which were able to be excited at ~800 nm. Minimized absorption of water as well as other biological constituents lies around this wavelength, producing a sweet exciting wavelength pot. In this nanosystem, Nd^{3+} acts as absorber to harvest 800 nm laser photons, while the Yb^{3+} ions play as bridging ions to accept the transferred energy from Nd^{3+} ions, and then sensitize the lanthanide activator (Er^{3+} or Tm^{3+}) to produce upconversion. They demonstrated that doping of a small proportion of Nd^{3+} concentration (e.g., 1%) was able to enhance upconversion more than 20 times when compared with conventional Yb^{3+}/Er^{3+} (or Tm^{3+}) codoped UCNPs under excitation at ~800 nm (Figure 8a,b).[43] Based on a similar mechanism, a core/shell structure was employed by Yan and co-workers to spatially isolate lanthanide ions to eliminate deleterious cross relaxations. Yb^{3+} and activators were codoped in the core, while the shell contains Nd^{3+} and Yb^{3+}. This design produces a similar UC efficiency when excited at ~808 nm excitation to the one when excited at ~980 nm. In vivo application of these UCNPs with minimized water heating phenomena were verified by them (Figure 8c).[44] Along this line, Liu and co-workers fabricated efficient core/shell UCNPs excitable at 795 nm by confining Nd^{3+} ions in both core and

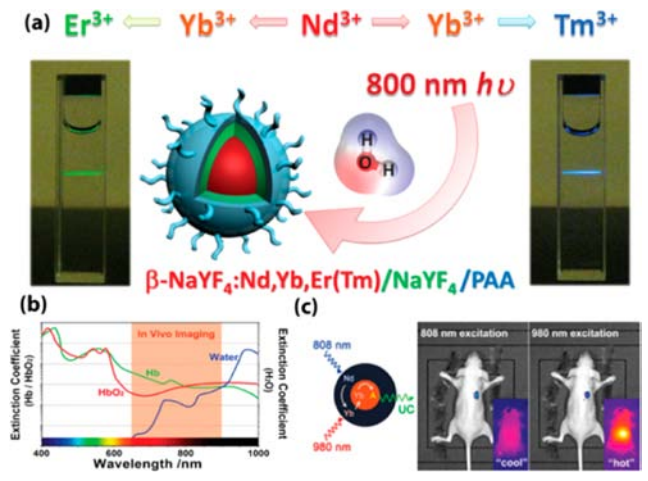

Figure 8. (a) Upconversion process of $Nd^{3+} \rightarrow Yb^{3+} \rightarrow Er^{3+}(Tm^{3+})$ tridopants system with 800 nm excitation. (b) Spectra profiles of tissue optical window. The extinction coefficient of water at 800 nm is about 20 timers lower than that at 980 nm (Hb: hemoglobin; HbO_2: oxyhemoglobin). (c) In vivo heating effect induced by laser irradiation with 808 and 980 nm. (Reprinted with permission from refs 39 and 40. Copyright 2013 John Wiley and Sons and 2013 American Chemical Society.)

dx.doi.org/10.1021/bc5003967 | Bioconjugate Chem. 2015, 26, 166−175

shell. Viability study of HeLa cells under 800 and 980 nm irradiation showed that almost all cells were killed when irradiated with 980 nm laser (5 min, 6 W/cm^2), while cells remained intact under identical conditions of 800 nm.[45]

5. UCNP-MEDIATED PHOTOCHEMISTRY AND PHOTOTHERAPY

5.1. UCNPs for Photoreaction. Light can act as a highly orthogonal external stimulus to manipulate photochemical reactions in a spatiotemporal manner. Photolysis of photoactivatable or "caged" molecules has been well proven to be one effective strategy for noninvasive regulation of biological activities and processes in living systems. This strategy involved the use of a light-sensitive linkage to introduce a caging moiety onto therapeutic or imaging agents, thus darkening their bioactivities. When delivered to an intended area, the use of light stimuli is able to photocleave the linkage, detach the caging moiety, and then recover the bioactive effects of the agents. As such, minimized bioactive side effects are achieved during the delivery process of agents.

In this regard, versatile photosensitive molecules have been developed. However, most photosensitive molecules are in need of ultraviolet (UV) light to produce photochemical reactions. An excessive exposure of living systems to such short-wavelength light can produce a phototoxic effect. Moreover, UV light can penetrate tissue only to a limited extent (<3 mm), limiting its use in vivo. Meanwhile, although multiphoton caging compounds have been developed under NIR light excitation, their low multiphoton absorption cross sections as well as the required use of an expensive ultrashort pulsed laser limit their use. Hence, an in situ generation of UV light utilizing nanoparticles with a biocompatible low-energy NIR excitation is fascinating, since it can spatiotemporally restrict photochemical reactions in the nanometer regime with minimal photodamage, and can produce significantly enhanced light penetration in tissue. Therefore, NIR-to-UV UCNPs can be selected as promising functional materials toward photoactivatable imaging.

One of the first demonstrations on UCNP induced photochemical reaction was reported in 2010 by Yan et al., who presented a prototype of rewritable 2D optical storage medium with a potential high-density recording capacity. The writing and erasing processes are provided by the regulation of switched optical properties of photochomic diarylethene with UC luminescence from ordered UCNP nanopatterns.[46] Then, Neil R. Branda et al. demonstrated photolysis of caged compounds from the generalized 3′,5′-dialkoxybenzoin by using NIR-to-UV UCNPs to yield a 2-phenylbenzo[*b*]furan and a carboxylic acid.[47]

In 2012, Xing et al. reported controlled photo-uncaging of D-luciferin from D-luciferin-conjugated NIR-to-UV UCNPs. The released D-luciferin can produce enhanced bioluminescence signals in deep tissue of a live mouse; low cellular damage is created due to the use of deeply penetrating biocompatible NIR light.[18] Similarly, they also presented a novel strategy for remote activation of platinum prodrug and for real-time imaging of apoptosis by encapsulating the photoactivatable PtIV prodrug and the caspase imaging peptide into silica-coated UCNPs. Upon NIR light irradiation, the converted UV UC emission from UCNPs@SiO_2 can activate the PtIV prodrug to produce potent antitumor cytotoxic effect in human ovarian carcinoma A2780 cells and in cisplatin-resistant variant A2780cis cells. Moreover, the caspase enzymes produced in apoptosis can effectively cleave the caged peptide to recover the luminescence of Cy5, thereby allowing the direct imaging of apoptosis in living cells.[48]

Moreover, our group reported on a new family of UCNPs with tunably enhanced NIR-to-UV upconversion. We observed that the upconverted UV emission can be monotonically increased with an increase of Yb^{3+} concentration while the enhancement of blue and NIR emissions was rather limited. The optimal α-$NaYbF_4$:Tm@CaF_2 core/shell UCNPs produce even stronger UV emissions than the well-established β-$NaYF_4$:30%Yb, 0.5%Tm@β-$NaYF_4$ core@shell nanoparticles. In addition, the CaF_2 shell is found to be more effective than typically used β -$NaYF_4$ shell in resisting quenching in aqueous medium to preserve the upconverted UV emissions. Furthermore, we demonstrated that the UV-emitting UCNPs can produce rapid in situ photoactivation in live cells under irradiation with a low-power NIR (975 nm) CW laser (Figure 9). These UV enhanced UCNPs offer an opportunity to serve as UV nanoilluminators for various biomedical applications, such as tracing cell lineages and probing protein dynamics. Moreover, this research improved our understanding of upconverting luminescence and accelerated the development of more efficient UV emitting UCNPs for a broad spectrum of biophotonic applications.[49]

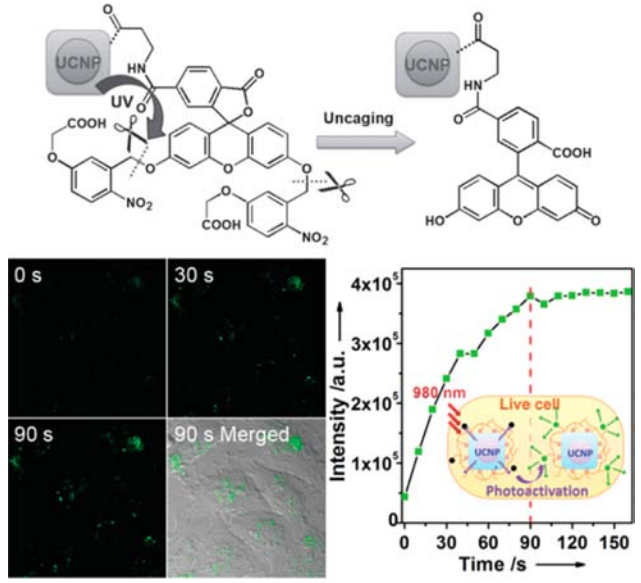

Figure 9. (top) NIR photoactivation process of caged fluorescein on UCNPs. (bottom) Photoactivation of cF-UCNPs in live HeLa cells by 975 nm laser confocal microscope scanning. (Reprinted with permission from ref 45. Copyright 2013 John Wiley and Sons.)

5.2. Photodynamic Therapy. Photodynamic therapy (PDT) is a clinical tumor treatment that uses light-generated cytotoxic singlet-state reactive oxygen species to kill tumors. This treatment is recognized as having minimal invasiveness and toxicity. Typical PDT treatments involve three components: the photosensitizer, the light source, and the oxygen within the tissue at the disease site. Conventional PDT is limited by the penetration depth of visible light needed for its activation. The involvement of UCNPs in PDT is of clinical significance, as it provides a new technique to treat tumors located in deep tissue. It relies on the fact that UCNPs can efficiently convert deeply penetrating NIR light to visible

dx.doi.org/10.1021/bc5003967 | Bioconjugate Chem. 2015, 26, 166−175

wavelengths that can excite photosensitizer to produce cytotoxic $^1O_2$.

A large amount of UCNP-photosensitizer systems have been developed by energy transfer from (blue, green, and red) UCNPs to photosensitizers with appropriate absorption. For example, $NaYF_4$:Yb,Tm nanoparticles were coated by a tris(bipyridine)ruthenium(II) ($Ru(bpy)_3^{2+}$), which has a maximum absorbance at 450 nm matching the blue emission of Tm^{3+}. Under 980 nm excitation, singlet oxygen ($^1O_2$ generation) was chemically demonstrated.[50] In addition, a new and efficient NIR photosensitizing nanoplatform for UC-PDT has been developed, based on red-emitting UCNPs. Three commonly used photosensitizers, including chlorine e6 (Ce6), zinc phthalocyanine (ZnPc), and methylene blue (MB), are simultaneously loaded onto the α-cyclodextrin-modified UCNPs to form Ps@UCNPs complexes. Efficient cytotoxic effects in cancer cells have been demonstrated under 980 nm NIR excitation.[51] More importantly, the first in vivo UCNP-based PDT was demonstrated by Liu et al. Therein, a FDA approved PDT drug [i.e., photosensitizing porphyrin derivative chlorine 6 (Ce6)] was noncovalently incorporated into PEGylated amphiphilic polymer-coated $NaYF_4$:Yb,Er nanoparticles. Excellent tumor regression was observed upon intra tumor injection with UCNP-Ce6 and laser irradiance with 980 nm cw laser.[52] Moreover, as opposed to previous use of single photosensitizer, Zhang et al. exploited the use of multicolor emission bands of the UCNPs for simultaneous activation of two photosensitizers to produce an enhanced PDT. Indeed, the combined use of two photosensitizers leads to a more efficient utilization of upconverted energy from UCNPs, thus collectively producing a greater PDT efficacy. In vivo studies showed effective tumor growth inhibition in PDT-treated mice either by direct injection of UCNPs into melanoma tumors or by intravenous injection of UCNPs conjugated with a tumor-targeting agent into tumor-bearing mice (Figure 10).[53]

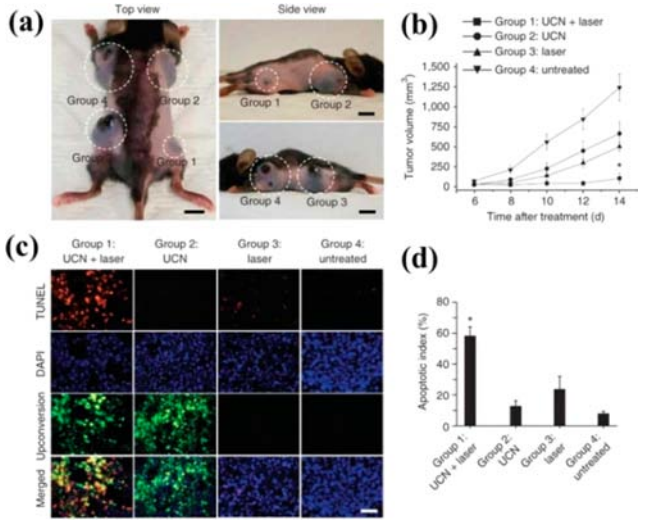

Figure 10. (a) Representative gross photos of a mouse showing tumors (highlighted by dashed white circles) at 14 d after treatment with the conditions described for groups 1−4. Scale bars, 10 mm. (b) Tumor volumes in the four treatment groups at 6, 8, 10, 12, and 14 d after treatment to determine the effectiveness of the treatment in terms of tumor cell growth inhibition. (c) TUNEL staining of tissue sections from the treatment groups at 24 h after treatment to determine the effectiveness of the treatment in terms of tumor cell death by apoptosis. DAPI counterstaining indicates the nuclear region, and upconversion fluorescence imaging indicates the position of the injected UCNP-labeled cell (400× magnification). Scale bar, 20 μm. (d) The apoptotic index charted as the percentage of TUNEL-positive apoptotic nuclei divided by the total number of nuclei visualized by counterstaining with DAPI obtained from counts of randomly chosen microscopic fields. (Reprinted with permission from ref 49. Copyright 2012 Nature Publishing Group.)

6. CONCLUSION AND PERSPECTIVES

In the past decade, many conceptual UCNP applications have been successfully presented to visualize both structural and functional information ranging from a single living cell level to a whole body of animal level. In addition, toxicity of these nanoparticles has been recently comprehensively reviewed, generally describing their cellular uptake, cytotoxicity, biodistribution, and in vivo excretion. Although further systematic examinations are required, the current results are quite encouraging and these UCNPs shows much less toxicity in vitro and in animal models (e.g., zebra fish) than QDs.[54,55] However, most of commercialized imaging equipment applicable for dyes and QDs is inappropriate for direct application to UCNPs due to their unique optical properties. Many research groups have to construct homemade instruments by their own endeavor, such as a 980 nm CW laser equipped confocal microscope and in vivo imaging box. Somehow the instrument problem has limited the popularity of UCNP-based bioprobes for biologists and clinicians, and slowed the process of commercialization. Fortunately, some instrument manufacturers have recently begun to accept customized orders for UCNP imaging, which is good news to the community of UCNPs.

On the other hand, despite their superior advantages when compared with conventional imaging probes of dyes or QDs, there still exist some important challenges for the community of UCNPs, mainly arising from the problems of UCNPs themselves. We have listed here some of these important challenges:

1. How to increase the upconversion efficiency of ultrasmall UCNPs. Besides traditional epitaxial core/shell strategy, is it possible to further improve the crystallinity and decrease the lattice defect by postsynthesis aging or calcination?
2. Despite much progress in material development, no single molecule imaging using UCNP in the context of cellular systems has been demonstrated. Is it possible to develop monofunctional UCNPs for protein conjugation? Since these UCNPs are not blinking, how can we confirm that what we observed are single identities?
3. Lanthanide doped UCNPs are hampered by the low absorption cross section and narrow excitation band. Zou et al. reported on an innovative strategy of employing organic dyes as light harvesting antennas to entail broadband excitation along with much more efficient light harvesting.[57] In their studies, NIR-absorbing cyanine dyes were linked to the nanoparticle surface via a carboxylic acid functional group. Dye antenna effects are capable of producing as high as ~3300-fold intensity UC enhancement when dispersing UCNPs in organic solvents. How can we incorporate this development in bioimaging?
4. Despite much progress in making sub 10 nm small lanthanide doped UCNPs, the impact of nanoparticle size on pharmacokinetics is largely unknown. Ultrasmall

dx.doi.org/10.1021/bc5003967 | Bioconjugate Chem. 2015, 26, 166−175

(~2 nm) $NaGdF_4$ nanodots have been developed by Bu and Shi et al. These nanoparticles were found to be removable from the animal through the urine.[56] Since UCNPs share a similar matrix, is it possible to make UCNPs possessing satisfactory renal clearance?

5. Development and application of 800 nm excited Nd-Yb-Er/Tm tridopant UCNPs in biomedical photoreactions is encouraging to overcome the potential water heating effects in 980 nm. Can we further improve the spatioresolution of the whole animal imaging? Can we eventually beat the photoacoustic or micro-CT, MRI in the clinical uses regarding the resolution?

AUTHOR INFORMATION

Corresponding Authors

*E-mail: Jie.Shen@umassmed.edu; Fax: +1 5088566231; Tel +1 5088563297.

*E-mail: Gang.Han@umassmed.edu.

Notes

The authors declare no competing financial interest.

ACKNOWLEDGMENTS

The authors thank the financial support from the start-up fund of the University of Massachusetts Medical School, a Worcester Foundation Mel Cutler Award, Human Frontier program, National Institutes of Health R01MH103133, and a UMass CVIP award and the China Scholarship Council (CSC).

REFERENCES

(1) Ntziachristos, V. (2010) Going deeper than microscopy: the optical imaging frontier in biology. *Nat. Methods 7*, 603−14.

(2) Xu, H., Li, Q., Wang, L., He, Y., Shi, J., Tang, B., and Fan, C. (2014) Nanoscale optical probes for cellular imaging. *Chem. Soc. Rev. 43*, 2650−61.

(3) Loening, A. M., Wu, A. M., and Gambhir, S. S. (2007) Red-shifted Renilla reniformis luciferase variants for imaging in living subjects. *Nat. Methods 4*, 641−3.

(4) Day, R. N., and Davidson, M. W. (2009) The fluorescent protein palette: tools for cellular imaging. *Chem. Soc. Rev. 38*, 2887−921.

(5) Michalet, X., Pinaud, F. F., Bentolila, L. A., Tsay, J. M., Doose, S., Li, J. J., Sundaresan, G., Wu, A. M., Gambhir, S. S., and Weiss, S. (2005) Quantum dots for live cells, in vivo imaging, and diagnostics. *Science 307*, 538−44.

(6) Achilefu, S. (2010) Introduction to concepts and strategies for molecular imaging. *Chem. Rev. 110*, 2575−8.

(7) Chen, G., Qiu, H., Prasad, P. N., and Chen, X. (2014) Upconversion nanoparticles: design, nanochemistry, and applications in theranostics. *Chem. Rev. 114*, 5161−214.

(8) Moerner, W. E. (2007) New directions in single-molecule imaging and analysis. *Proc. Natl. Acad. Sci. U. S. A. 104*, 12596−602.

(9) Wang, F., and Liu, X. (2009) Recent advances in the chemistry of lanthanide-doped upconversion nanocrystals. *Chem. Soc. Rev. 38*, 976−89.

(10) Bouzigues, C., Gacoin, T., and Alexandrou, A. (2011) Biological applications of rare-earth based nanoparticles. *ACS Nano 5*, 8488−505.

(11) Wang, F., Banerjee, D., Liu, Y., Chen, X., and Liu, X. (2010) Upconversion nanoparticles in biological labeling, imaging, and therapy. *Analyst 135*, 1839−54.

(12) Gnach, A., and Bednarkiewicz, A. (2012) Lanthanide-doped up-converting nanoparticles: Merits and challenges. *Nano Today 7*, 532−563.

(13) Campagnola, P. J., and Loew, L. M. (2003) Second-harmonic imaging microscopy for visualizing biomolecular arrays in cells, tissues and organisms. *Nat. Biotechnol. 21*, 1356−60.

(14) Zhou, J., Liu, Z., and Li, F. (2012) Upconversion nano-phosphors for small-animal imaging. *Chem. Soc. Rev. 41*, 1323−49.

(15) Wang, F., Han, Y., Lim, C. S., Lu, Y., Wang, J., Xu, J., Chen, H., Zhang, C., Hong, M., and Liu, X. (2010) Simultaneous phase and size control of upconversion nanocrystals through lanthanide doping. *Nature 463*, 1061−5.

(16) Heer, S., Kompe, K., Gudel, H. U., and Haase, M. (2004) Highly efficient multicolour upconversion emission in transparent colloids of lanthanide-doped NaYF4 nanocrystals. *Adv. Mater. 16*, 2102−+.

(17) Haase, M., and Schafer, H. (2011) Upconverting nanoparticles. *Angew. Chem., Int. Ed. 50*, 5808−29.

(18) Auzel, F. (2004) Upconversion and anti-Stokes processes with f and d ions in solids. *Chem. Rev. 104*, 139−73.

(19) Mai, H. X., Zhang, Y. W., Si, R., Yan, Z. G., Sun, L. D., You, L. P., and Yan, C. H. (2006) High-quality sodium rare-earth fluoride nanocrystals: controlled synthesis and optical properties. *J. Am. Chem. Soc. 128*, 6426−36.

(20) Li, Z., and Zhang, Y. (2008) An efficient and user-friendly method for the synthesis of hexagonal-phase NaYF(4):Yb, Er/Tm nanocrystals with controllable shape and upconversion fluorescence. *Nanotechnology 19*, 345606.

(21) Bogdan, N., Vetrone, F., Ozin, G. A., and Capobianco, J. A. (2011) Synthesis of ligand-free colloidally stable water dispersible brightly luminescent lanthanide-doped upconverting nanoparticles. *Nano Lett. 11*, 835−40.

(22) Rantanen, T., Jarvenpaa, M. L., Vuojola, J., Kuningas, K., and Soukka, T. (2008) Fluorescence-quenching-based enzyme-activity assay by using photon upconversion. *Angew. Chem., Int. Ed. 47*, 3811−3.

(23) Zhou, H. P., Xu, C. H., Sun, W., and Yan, C. H. (2009) Clean and flexible modification strategy for carboxyl/aldehyde-functionalized upconversion nanoparticles and their optical applications. *Adv. Funct. Mater. 19*, 3892−3900.

(24) Wu, S., Han, G., Milliron, D. J., Aloni, S., Altoe, V., Talapin, D. V., Cohen, B. E., and Schuck, P. J. (2009) Non-blinking and photostable upconverted luminescence from single lanthanide-doped nanocrystals. *Proc. Natl. Acad. Sci. U. S. A. 106*, 10917−21.

(25) Yang, Y., Shao, Q., Deng, R., Wang, C., Teng, X., Cheng, K., Cheng, Z., Huang, L., Liu, Z., Liu, X., and Xing, B. (2012) In vitro and in vivo uncaging and bioluminescence imaging by using photocaged upconversion nanoparticles. *Angew. Chem., Int. Ed. 51*, 3125−9.

(26) Wang, L., Yan, R., Huo, Z., Zeng, J., Bao, J., Wang, X., Peng, Q., and Li, Y. (2005) Fluorescence resonant energy transfer biosensor based on upconversion-luminescent nanoparticles. *Angew. Chem., Int. Ed. 44*, 6054−7.

(27) Nam, S. H., Bae, Y. M., Park, Y. I., Kim, J. H., Kim, H. M., Choi, J. S., Lee, K. T., Hyeon, T., and Suh, Y. D. (2011) Long-term real-time tracking of lanthanide ion doped upconverting nanoparticles in living cells. *Angew. Chem., Int. Ed. 50*, 6093−7.

(28) Ostrowski, A. D., Chan, E. M., Gargas, D. J., Katz, E. M., Han, G., Schuck, P. J., Milliron, D. J., and Cohen, B. E. (2012) Controlled synthesis and single-particle imaging of bright, sub-10 nm lanthanide-doped upconverting nanocrystals. *ACS Nano 6*, 2686−92.

(29) Gargas, D. J., Chan, E. M., Ostrowski, A. D., Aloni, S., Altoe, M. V., Barnard, E. S., Sanii, B., Urban, J. J., Milliron, D. J., Cohen, B. E., and Schuck, P. J. (2014) Engineering bright sub-10-nm upconverting nanocrystals for single-molecule imaging. *Nat. Nanotechnol. 9*, 300−5.

(30) Zhao, J., Jin, D., Schartner, E. P., Lu, Y., Liu, Y., Zvyagin, A. V., Zhang, L., Dawes, J. M., Xi, P., Piper, J. A., Goldys, E. M., and Monro, T. M. (2013) Single-nanocrystal sensitivity achieved by enhanced upconversion luminescence. *Nat. Nanotechnol. 8*, 729−34.

(31) Wang, F., and Liu, X. (2014) Multicolor tuning of lanthanide-doped nanoparticles by single wavelength excitation. *Acc. Chem. Res. 47*, 1378−85.

(32) Chen, G. Y., Qiu, H. L., Fan, R. W., Hao, S. W., Tan, S., Yang, C. H., and Han, G. (2012) Lanthanide-doped ultrasmall yttrium fluoride nanoparticles with enhanced multicolor upconversion photoluminescence. *J. Mater. Chem. 22*, 20190−20196.

(33) Tian, G., Gu, Z., Zhou, L., Yin, W., Liu, X., Yan, L., Jin, S., Ren, W., Xing, G., Li, S., and Zhao, Y. (2012) Mn2+ dopant-controlled synthesis of NaYF4:Yb/Er upconversion nanoparticles for in vivo imaging and drug delivery. *Adv. Mater. 24*, 1226−31.
(34) Chatterjee, D. K., Rufaihah, A. J., and Zhang, Y. (2008) Upconversion fluorescence imaging of cells and small animals using lanthanide doped nanocrystals. *Biomaterials 29*, 937−43.
(35) Wang, M., Mi, C. C., Wang, W. X., Liu, C. H., Wu, Y. F., Xu, Z. R., Mao, C. B., and Xu, S. K. (2009) Immunolabeling and NIR-excited fluorescent imaging of HeLa cells by using NaYF(4):Yb,Er upconversion nanoparticles. *ACS Nano 3*, 1580−6.
(36) Nyk, M., Kumar, R., Ohulchanskyy, T. Y., Bergey, E. J., and Prasad, P. N. (2008) High contrast in vitro and in vivo photoluminescence bioimaging using near infrared to near infrared upconversion in Tm^{3+} and Yb^{3+} doped fluoride nanophosphors. *Nano Lett. 8*, 3834−8.
(37) Chen, G., Ohulchanskyy, T. Y., Kumar, R., Agren, H., and Prasad, P. N. (2010) Ultrasmall monodisperse NaYF(4):Yb(3+)/Tm(3+) nanocrystals with enhanced near-infrared to near-infrared upconversion photoluminescence. *ACS Nano 4*, 3163−8.
(38) Chen, G., Shen, J., Ohulchanskyy, T. Y., Patel, N. J., Kutikov, A., Li, Z., Song, J., Pandey, R. K., Agren, H., Prasad, P. N., and Han, G. (2012) alpha-NaYbF4:Tm(3+))/CaF2 core/shell nanoparticles with efficient near-infrared to near-infrared upconversion for high-contrast deep tissue bioimaging. *ACS Nano 6*, 8280−7.
(39) Liu, C., Gao, Z., Zeng, J., Hou, Y., Fang, F., Li, Y., Qiao, R., Shen, L., Lei, H., Yang, W., and Gao, M. (2013) Magnetic/upconversion fluorescent $NaGdF_4$:Yb,Er nanoparticle-based dual-modal molecular probes for imaging tiny tumors in vivo. *ACS Nano 7*, 7227−40.
(40) Sun, Y., Zhu, X., Peng, J., and Li, F. (2013) Core-shell lanthanide upconversion nanophosphors as four-modal probes for tumor angiogenesis imaging. *ACS Nano 7*, 11290−300.
(41) Esipova, T. V., Ye, X., Collins, J. E., Sakadzic, S., Mandeville, E. T., Murray, C. B., and Vinogradov, S. A. (2012) Dendritic upconverting nanoparticles enable in vivo multiphoton microscopy with low-power continuous wave sources. *Proc. Natl. Acad. Sci. U. S. A. 109*, 20826−31.
(42) Ni, D., Zhang, J., Bu, W., Xing, H., Han, F., Xiao, Q., Yao, Z., Chen, F., He, Q., Liu, J., Zhang, S., Fan, W., Zhou, L., Peng, W., and Shi, J. (2014) Dual-targeting upconversion nanoprobes across the blood-brain barrier for magnetic resonance/fluorescence imaging of intracranial glioblastoma. *ACS Nano 8*, 1231−42.
(43) Shen, J., Chen, G. Y., Vu, A. M., Fan, W., Bilsel, O. S., Chang, C. C., and Han, G. (2013) Engineering the upconversion nanoparticle excitation wavelength: cascade sensitization of tri-doped upconversion colloidal nanoparticles at 800 nm. *Adv. Opt. Mater. 1*, 644−650.
(44) Wang, Y. F., Liu, G. Y., Sun, L. D., Xiao, J. W., Zhou, J. C., and Yan, C. H. (2013) Nd(3+)-sensitized upconversion nanophosphors: efficient in vivo bioimaging probes with minimized heating effect. *ACS Nano 7*, 7200−6.
(45) Xie, X., Gao, N., Deng, R., Sun, Q., Xu, Q. H., and Liu, X. (2013) Mechanistic investigation of photon upconversion in Nd(3+)-sensitized core-shell nanoparticles. *J. Am. Chem. Soc. 135*, 12608−11.
(46) Zhang, C., Zhou, H. P., Liao, L. Y., Feng, W., Sun, W., Li, Z. X., Xu, C. H., Fang, C. J., Sun, L. D., Zhang, Y. W., and Yan, C. H. (2010) Luminescence modulation of ordered upconversion nanopatterns by a photochromic diarylethene: rewritable optical storage with non-destructive readout. *Adv. Mater. 22*, 633−7.
(47) Carling, C. J., Nourmohammadian, F., Boyer, J. C., and Branda, N. R. (2010) Remote-control photorelease of caged compounds using near-infrared light and upconverting nanoparticles. *Angew. Chem., Int. Ed. 49*, 3782−5.
(48) Min, Y., Li, J., Liu, F., Yeow, E. K., and Xing, B. (2014) Near-infrared light-mediated photoactivation of a platinum antitumor prodrug and simultaneous cellular apoptosis imaging by upconversion-luminescent nanoparticles. *Angew. Chem., Int. Ed. 53*, 1012−6.
(49) Shen, J., Chen, G., Ohulchanskyy, T. Y., Kesseli, S. J., Buchholz, S., Li, Z., Prasad, P. N., and Han, G. (2013) Tunable near infrared to ultraviolet upconversion luminescence enhancement in (alpha-$NaYF_4$:Yb,Tm)/CaF_2 core/shell nanoparticles for in situ real-time recorded biocompatible photoactivation. *Small 9*, 3213−7.
(50) Guo, Y., Kumar, M., and Zhang, P. (2007) Nanoparticle-based photosensitizers under CW infrared excitation. *Chem. Mater. 19*, 6071−6072.
(51) Tian, G., Ren, W. L., Yan, L., Jian, S., Gu, Z. J., Zhou, L. J., Jin, S., Yin, W. Y., Li, S. J., and Zhao, Y. L. (2013) Red-emitting upconverting nanoparticles for photodynamic therapy in cancer cells under near-infrared excitation. *Small 9*, 1929−1938.
(52) Wang, C., Tao, H., Cheng, L., and Liu, Z. (2011) Near-infrared light induced in vivo photodynamic therapy of cancer based on upconversion nanoparticles. *Biomaterials 32*, 6145−54.
(53) Idris, N. M., Gnanasammandhan, M. K., Zhang, J., Ho, P. C., Mahendran, R., and Zhang, Y. (2012) In vivo photodynamic therapy using upconversion nanoparticles as remote-controlled nanotransducers. *Nat. Med. 18*, 1580−5.
(54) Sun, Y., Feng, W., Yang, P., Huang, C., Li, F. The biosafety of lanthanide upconversion nanomaterials. *Chem. Soc. Rev.* [Online early access] DOI:10.1039/c4cs00175c.
(55) Gnach, A., Lipinski, T., Bednarkiewicz, A., Rybaka, J., Capobianco, J. A. Upconverting nanoparticles: assessing the toxicity. *Chem. Soc. Rev.* [Online early access] DOI: 10.1039/c4cs00177j.
(56) Xing, H., Zhang, S., Bu, W., Zheng, X., Wang, L., Xiao, Q., Ni, D., Zhang, J., Zhou, L., Peng, W., Zhao, K., Hua, Y., and Shi, J. (2014) Ultrasmall NaGdF4 nanodots for efficient MR angiography and atherosclerotic plaque imaging. *Adv. Mater. 26*, 3867−3872.
(57) Zou, W. Q., Visser, C., Maduro, J. A., Pshenichnikov, M. S., and Hummelen, J. C. (2012) Broadband dye-sensitized upconversion of near-infrared light. *Nat. Photonics 6*, 560−564.